Final Young Investigator Award Report

Prepared for The Cancer Research Foundation

3/31/15

Steffen Sammet, MD, PhD, DABR

Associate Professor of Radiology and Medical Physics

Thank you to the Cancer Research Foundation for its support of my work, titled: High Intensity Focused Ultrasound Ablation of Prostate Tissue in vivo with Magnetic Resonance Imaging Guidance. Thanks to your support, I have recently submitted a manuscript for review. This manuscript describes in great detail the results of my work for the Young Investigator Award from the Cancer Research Foundation. I have attached this manuscript in the hope that you will accept it as my final report for my CRF Young Investigator Award.

Cavernosal Nerve Functionality Evaluation after MRI-Guided Transurethral Ultrasound Treatment of the Prostate

Running title: MRI-guided Transurethral Ultrasound Therapy of the Prostate in-vivo

Steffen Sammet, M.D., Ph.D. [1,2], Ari Partanen, Ph.D. [3], Ambereen Yousuf, M.D. [1], Christina Sammet, Ph.D. [4], Emily V. Ward, M.D. [1], Craig Wardrip, M.D. [5], Marek Niekrasz, M.D. [5], Tatjana Antic, M.D. [6], Aria Razmaria, M.D. [5], Keyvan Farahani, M.D.[7], Shunmugavelu Sokka, Ph.D. [3], Gregory Karczmar, Ph.D.[1,2], Aytekin Oto, M.D.[1]

[1] Department of Radiology, University of Chicago, Chicago, IL, 60615, USA

[2] Committee on Medical Physics, University of Chicago, Chicago, IL, 60615, USA

[3] Philips Healthcare, Cleveland, OH 44143, USA

[4]Department of Medical Imaging, Lurie Children's Hospital, Chicago, IL 60611, USA

[5] Department of Surgery, University of Chicago, Chicago, IL 60615, USA

[6] Department of Pathology, University of Chicago, Chicago, IL 60615, USA

[7] National Cancer Institute, Bethesda, MD 60615, USA

Author Contributions:

Dr. Steffen Sammet, Dr. Ari Partanen, Dr. Ambereen Yousuf, Dr. Keyvan Farahani, Dr. Shunmugavelu Sokka, Dr. Gregory Karczmar and Dr. Aytekin Oto designed the research; Dr. Steffen Sammet, Dr. Ari Partanen, Dr. Gregory Karczmar and Dr. Aytekin Oto developed the MRI protocols; Dr. Steffen Sammet, Dr. Ari Partanen and Dr. Aytekin Oto performed the MRI and therapeutic ultrasound experiments; Dr. Tatjana Antic performed the histological analysis and the histological/radiological comparison; Dr. Aytekin Oto performed the radiological image analysis and the histological/radiological comparison; Dr. Steffen Sammet, Dr. Craig Wardrip, Dr. Marek Niekrasz and Dr. Aria Razmaria monitored the animals during therapeutic ultrasound treatment and performed surgeries; Dr. Steffen Sammet, Dr. Ari Partanen, Dr. Ambereen Yousuf, Dr. Emily Ward, Dr. Christina Sammet, and Dr. Aytekin Oto wrote the paper.

Supportive Foundations:

This project has been funded in part by the National Cancer Institute Education and Career Development program R25 Cancer Nanotechnology in Imaging and Radiotherapy (5R25CA132822-04), the Cancer Research Foundation, the University of Chicago Comprehensive Cancer Center and Philips Healthcare.

Correspondence to:

Steffen Sammet, M.D., Ph.D., DABR, FAMP

Associate Professor and Director of Clinical MR Physics

Department of Radiology, Committee on Medical Physics and Comprehensive Cancer Center

University of Chicago Medicine

5841 South Maryland Avenue, MC2026

Chicago, Illinois 60637

Email: ssammet@uchicago.edu

Telephone and Fax:

Tel: +1(773) 702-3162

Fax: +1(773) 702-1161

Ethics Related Statements:

Institutional review board statement: The study was reviewed and approved by the University of Chicago Institutional Animal Care and Use Committee.

Clinical trial registration: This study is not a registered clinical trial.

Informed consent statement: This study did not involve human subjects and therefore did not require informed consent.

Biostatistics: The paper describes a feasibility study with qualitative results and therefore biostatistical analysis was not performed.

Conflict-of-Interest Statement: Steffen Sammet, M.D., Ph.D. has received research funding from Philips Healthcare. Ari Partanen, Ph.D. is an employee of Philips Healthcare. Shunmugavelu Sokka, Ph.D. is an employee of Philips Healthcare. Aytekin Oto, M.D. has received research funding from Philips Healthcare and fees as a consultant for Guerbet SA.

Data Sharing Statement: No additional data are available.

Abstract

AIM

To evaluate the feasibility of using therapeutic ultrasound as an alternative treatment option for organ-confined prostate cancer.

METHODS

In this study, a trans-urethral therapeutic ultrasound applicator in combination with 3T Magnetic Resonance Imaging (MRI) guidance was used for real-time multi-planar MRI-based temperature monitoring and temperature feedback control. We evaluated the feasibility and safety of MRI-guided trans-urethral ultrasound to effectively and accurately ablate prostate tissue while minimizing the damage to surrounding tissues in eight canine prostates. MRI was used to plan sonications, monitor temperature changes during therapy, and to evaluate treatment outcome. Real-time temperature and thermal dose maps were calculated using the proton resonance frequency shift technique and were displayed as two-dimensional color-coded overlays on top of the anatomical images. After ultrasound treatment, an evaluation of the integrity of cavernosal nerves was performed during prostatectomy with a nerve stimulator that measured tumescence response quantitatively and indicated intact cavernous nerve functionality. The spatio-temporal accuracy was correlated to pre-defined MRI ablation volumes and corresponding histo-pathological sections after prostatectomy.

RESULTS

A total of 16 sonications were performed in 8 canines. Initial planning images enabled identification of the prostate and prescription of sonication locations in all canines. Temperature elevations corresponded within 1 degree of the targeted sonication angle, as well as with the width and length of the active transducer elements. All sonications were stopped automatically after control point target temperature (56°C) was reached. In all canines erectile responses were evaluated with a cavernous nerve stimulator post-treatment and showed a tumescence response after stimulation with an electric current. These results indicated intact cavernous nerve functionality. In all specimens, regions of

thermocoagulation were detected and noted to be within the prostate capsule, with no thermal damage to the peri-prostatic tissues. Ablated volumes defined by cumulative thermal dose and volumes identified on post-procedural contrast-enhanced MRI demonstrated excellent correlation on visual analysis. All of the ablation zones received a consensus score of 3 (excellent) for the location and size of the correlation between the histologic ablation zone and MRI based ablation zone. During the prostatectomy and histologic examination, no damage was noted in the bladder and rectum.

CONCLUSION

MRI-guided trans-urethral ultrasound therapy of the prostate has potential to accurately ablate prostatic regions, while minimizing the morbidities associated with conventional whole-gland resection or therapy.

Keywords: thermal ablation, therapeutic ultrasound, thermotherapy, minimally invasive, magnetic resonance imaging, image-guided therapy, intra-operative, histology, validation

Core Tip: Therapeutic ultrasound is a promising treatment for minimally invasive tissue ablation. This study assed a novel Magnetic Resonance Imaging (MRI) guided trans-urethral ultrasound to ablate canine prostate tissue in-vivo. 3T MRI was used for real-time temperature monitoring and thermotherapy feedback control. Post-treatment evaluation of cavernous nerve functionality was performed with a nerve stimulator. Treatment accuracy was assessed by correlation of planning and histo-pathological results. Regions of thermocoagulation were contained within the capsule, with no thermal damage to the peri-prostatic tissues. These results indicate that MRI-guided ultrasound therapy can accurately ablate prostatic regions with minimal damage to surrounding tissue.

Introduction

Prostate cancer (Pca) is the second most common cancer and among the leading causes of cancer deaths in men in the US[1]. Overtreatment is described as an unnecessary aggressive treatment of Pca including prostatectomy and radiation therapy and can lead to complications. The overtreatment of Pca is an important public health problem occurring in about 30-40% of the cases[2]. There is a growing interest in focal treatment strategies for Pca that could achieve comparable oncologic efficacy with minimal adverse effects on sexual and urinary function [3, 4].

High intensity focused ultrasound (HIFU) treatment is a novel minimal invasive treatment option where an ultrasound probe emits a beam of ultrasound, which is focused to reach a high intensity in the target area. Absorption of the ultrasound energy creates an increase in temperature and destroys tissue when the temperature exceeds ≥56°C within the focal area; a phenomenon defined as thermo-ablation [4-8]. Ultrasound therapy may be employed with ultrasound (US) or magnetic resonance imaging (MRI) guidance. MRI is superior to diagnostic US due to its ability to better detect Pca, monitor real-time temperature changes in multiple planes and for prediction of the extent of tissue destruction using sequences such as dynamic contrast-enhanced MRI (DCE-MRI) and diffusion-weighted imaging (DWI) in the post-ablation setting[9-11]. A combination of therapeutic ultrasound and MR guidance is particularly beneficial for focal and regional therapy of Pca [8]. Preliminary clinical trials utilizing trans-rectal and trans-urethral HIFU for focal ablation of Pca have reported feasibility of these techniques [6, 12]. One of the important side effects of whole gland treatment is erectile dysfunction. Even though, focal therapy is expected to be safer in this regard, there is limited data in the literature to support this hypothesis.

In our study, a novel transurethral ultrasound therapy device combined with real-time multi-plane MRI based temperature monitoring and temperature feedback control, was tested in a preclinical canine study[13]. The goal was in-vivo evaluation of the safety of this transurethral ultrasound therapy device. In addition to the rectal damage, we

specifically assessed the post-treatment functionality of the cavernosal nerves by analyzing the tumescence response qualitatively and quantitatively with a nerve stimulator during prostatectomy.

Materials and Methods

Animals

In this Institutional Animal Care and Use Committee (IACUC) approved [University of Chicago, IACUC protocol number: 72317] MRI guided ultrasound treatment study, eight canines (age range: 6 to 57 months, average age: 26 months; weight range 24 kg to 35.8 kg average weight: 27.9 kg) were treated with therapeutic ultrasound.

Pre-treatment procedures

A perineal urethrostomy was performed a week before the HIFU treatment in all canines to better accommodate the ultrasound applicator in the curvature of the canine penile urethra. The canines were sedated before ultrasound treatment using IM acepromazine (10 mg/ml) and hydromorphone (2 mg/ml) followed by cephalic IV catheterization. Anesthesia was induced with Propofol (10 mg/kg) and the canines were intubated. The anesthesia was maintained with a continuous inhalation of isoflurane (2-4%) for the ultrasound treatment. A 6-french Foley catheter was placed to empty the bladder until treatment. A 20-french rectal tube was placed before the ultrasound treatment to release gases from the rectum. The ultrasound applicator was carefully manually advanced to the level of the prostate and the correct position in the prostate was checked with MR imaging. An experienced veterinary team monitored each canine throughout the procedure continuously. Monitoring included an ECG, blood pressure, blood oxygenation, in- and expired gases and physiological saline infusion.

MR-guided ultrasound therapy system

A prototype MR-guided ultrasound therapy system (Philips Healthcare, Vantaa, Finland) with temperature feedback was utilized for administration of the ultrasound exposures (sonications) on a clinical 3T MRI system (Achieva, Philips Healthcare, Cleveland). The ultrasound therapy system included a therapy control workstation with a planning software, a radio-frequency generator, a rigid, water-cooled trans-

urethral ultrasound applicator (5 mm [15 French] diameter) with eight transducer elements (4 mm × 5 mm/element) (Fig. 1) and a motor unit enabling rotation of the applicator (Fig. 2). A standard 8-channel SENSE cardiac receiver MR coil (Philips Healthcare, Best, The Netherlands) was used for treatment planning, temperature mapping, and post-treatment imaging (Fig. 3). The coil consisted of a 4-element anterior and a 4-element posterior part and was immobilized with straps around the canine and on the patient table (Fig. 4).

Sonications were performed in continuous wave mode at 6.0 MHz. The applicator rotated about its long axis, with ultrasound beams propagating into the target tissue through a thin (25 μm) cylindrical polyester membrane. Acoustic coupling was achieved using ultrasound gel. Cooling of the anatomic near field (in this case the urethra) was achieved by means of a closed loop circuit of flowing room temperature degassed water between the transducer elements and membrane. Adjusting the output power, sonication duration, and number of active transducer elements controlled ablation depths from the urethra and ablation volumes.

Treatment planning and MR thermometry

MRI was used to plan sonications, monitor temperature changes during therapy, and to evaluate treatment outcome. Thermal dose (e.g. cumulative equivalent minutes at 43°C [CEM_{43}]) was used to quantify thermal damage to tissue, and dose >240 CEM_{43} was used to indicate ablative exposures [14]. T_2-weighted Turbo Spin Echo (TSE) images used for treatment planning were acquired as 2D multi-slice stacks in coronal, sagittal, and axial planes. Temperature elevations during ultrasound therapy were monitored using rapid multi-planar MR thermometry. Seven axial slices and one sagittal slice were acquired with a spatial resolution of 1.5 × 1.5 × 5 mm^3 for each dynamic cycle resulting in a temporal update rate of 4.1 seconds / 8 slices. The slices were positioned parallel to the ultrasound beams, allowing for temperature monitoring and thermal dose calculations at the target as well as in surrounding tissues. Real-time temperature and thermal dose maps were calculated using the proton resonance frequency shift (PRFS,

0.0094 ppm/°C) technique [15] and displayed as two-dimensional color-coded overlays on top of the anatomical images. Temperature maps were corrected for baseline drift by subtracting the average apparent temperature change of all voxels in a freehand-drawn reference region (axial slice) in nearby muscle, outside the heated region.

Following ultrasound therapy, the axial T_2-weighted images were reacquired, followed by a T_1-weighted fast-field echo (T_1-FFE) sequence using clinically approved gadolinium-based contrast agent (Multihance, 0.1 mmol/kg). 2D multi-slice DWI was also performed prior to contrast agent injection. Previous studies have validated the use of both DCE-MRI and DWI to visualize necrotic tissue[16, 17].

Ablation feedback control

Before ablations, a test-sonication (P_{ac} = 1.1 W / channel, 1-3 active elements, t = 10-20 s) was performed to confirm transducer angle, location of heating, and the quality of acoustic coupling. Between sonications, the transducer was rotated to the next position using control software, and a cool down period (>10 min) was employed to ensure return to baseline temperature. This heat and cool cycle was repeated two times (two discrete locations) in each canine prostate.

Point targets were intentionally selected in the prostatic central zone, transitional zone and peripheral zone, in order to assess the feasibility of ablation in these locations. Temperature feedback was used to control ablation in the target region. A single control point (5 voxels) provided temperature feedback at a user-defined radial distance from the applicator (1.3 cm to 1.9 cm, depending on the size of the prostate). The power level was kept constant for all independent sonications (range = 1.1 W to 1.8 W acoustic power / channel) and sonication was automatically stopped when mean temperature in this control point reached 56°C[18].

Evaluation of the integrity of cavernosal nerves post-treatment

Following the procedure, during the prostatectomy to harvest the prostate, CaverMap Surgical Aid (Blue Torch Corporation, Norwood, MA) was used intra-operatively to identify and map the integrity of cavernosal nerves responsible for potency (Fig. 5)[19].

The CaverMap Surgical Aid combines a nerve stimulator with an erectile response detection system for intraoperative use. This system consists of three major components:

1. The control unit, which contains the digital and analog electronics, adjustable controls, user interface, and connectors for the probe handle and disposable kit.
2. The probe handle, which is sterile and reusable, is the component that allows the surgeon to control the device intraoperatively.
3. The disposable kit, which contains items for onetime use, is made up of the probe tip that attaches to the probe handle, the tumescence sensor, and the lead that connects the sensor to the control unit. The electrode containing probe tip emits the electrical current

The system applies a mild electrical stimulation for a measured tumescence response. The probe tip was placed on tissues that are suspected to contain cavernous nerves (Fig. 6 and Fig. 7). Stimulation was accomplished by inducing a biphasic current pulse train for up to 80 seconds with a controlled current intensity (8 mA to 20 mA) and pulse duration of 800 microseconds. The device was programmed to provide a gradual increase in current from 8 to 20 mA in 20-second increments. When the tissue is stimulated, erectile responses are detected in the form of changes in penile circumference in a previously placed tumescence sensor loop around the canine's penis. A small erectile response in the form of an increase or decrease in penile girth is produced. A full erection is not achieved for two reasons: (1) only external nerve stimulation is used, (2) other coordinated signals and changes in vasculature are usually required for a normal erection. Based on the presence or absence of a confirmed response, the course of the cavernous nerves was mapped and the functional state of the cavernous nerves after the ultrasound procedure was evaluated. Changes in penile circumference were electronically detected and displayed as relative change, with both visible and audible displays (light-emitting diode [LED] scale and changes in a tone, respectively) (Fig. 8).

The penile sensor contains a small amount of mercury that allows measurement of electric resistance to the supplied current. As the penile circumference changes, so does the length of mercury in the sensor loop, which is reflected in minute changes in resistance. Minimal changes in tumescence of 0.5% are considered positive responses to nerve stimulation. To avoid exhausting the erectile response, stimulation is discontinued once an unequivocal response is reached, with no attempt to determine maximal responses with higher current intensity[20].

Post-treatment procedures

Following treatment and caver-mapping, canines were euthanized using IV injection of sodium pentobarbital (150 mg/kg) followed by prostatic tissue procurement. To assess thermal damage to pelvic tissue, sections of muscle, rectum, and fat around the prostate were also resected during procurement (Fig. 9) and sent for histological analysis (Fig. 10).

Histopathological analysis

Following resection, prostates were fixed in 10% formalin for 24 hours. Using the mold, the prostate was then sliced every 3 mm to achieve congruence with MRI axial slices (acquired with 1 mm spacing/thickness). Subsequently, specimens were placed in 10% formalin and sent for cytokeratin-8 (CK8) and hematoxylin and eosin (H&E) staining. On histology, cell viability was measured using vital stain CK8 (CAM 5.2)[21, 22]. Areas of non-viable cells were marked with absence of stain. Formalin-fixed prostate slices were photographed and routinely processed, paraffin-embedded, and sectioned at 5 μm. Step sections at 3 mm intervals were taken of slices showing grossly visible lesions (Fig. 10).

Treatment analysis

Sonication data analysis was performed on the ultrasound treatment therapy console. The mean temperature at the control point and the maximum temperature within the heated region of the prostate were analyzed from the axial slices of MR thermometry

images. Furthermore, thermal dose (>240 CEM_{43}) volumes were calculated according to the Sapareto-Dewey equation[23]. Temperature map mean noise level was calculated as time-averaged temperature standard deviation in an unheated region.

Non-perfused volumes on immediate post-ablation DCE-MRI images were visually correlated with whole-mount sections of the prostate by an experienced genitourinary pathologist and radiologist. In each case, the correlation between MRI and pathology for location and size of the ablation zone was separately scored on a scale of 3 (no correlation: 1; modest correlation: 2; and excellent correlation: 3).

Results

MR-Imaging

MRI was used for treatment planning and temperature monitoring (Fig. 11). Initial planning images enabled identification of the prostate and prescription of sonication locations (Fig. 11 a, Fig. 12 a and b). Temperature elevations (Fig. 11 b, c) corresponded within 1 degree of the targeted sonication angle, as well as with the width and length of the active transducer elements. Temperature maps had a mean noise level of 0.3°C ± 0.1°C. Fig. 11 d shows a corresponding histological slide of the canine prostate in haematoxylin and eosin staining to evaluate HIFU treatment effects.

Ablation feedback control

A total of 16 sonications were performed in 8 canines. All sonications were stopped automatically after control point target temperature (56°C) was reached. Trans-urethral ultrasound therapy with MRI guidance enabled multi-planar temperature monitoring in the prostate as well as in surrounding tissues allowed for safe, targeted, and controlled ablations of prescribed volumes.

Sonications resulted in temperature elevations with the major axis in the direction of the ultrasound beam propagation. Mean temperature within the control point, and maximum temperature within the heated region ($\Delta T>2°C$) are shown in Fig. 11 b, c. For all feedback-controlled sonications, the mean time required to achieve target temperature (56°C) at the control depended on the control point distance, applied power, and local tissue characteristics, at which point the temperature feedback algorithm appropriately stopped the sonication. Upon sonication completion, temperature returned to baseline levels after 3-5 minutes. Agreement of temperature before and after sonication suggests that the magnetic drift correction was correctly applied in order to obtain accurate thermal maps.

Thermal dose estimation, image analysis, and histopathological analysis

Representative examples of contrast-enhanced MR-image, temperature maps and

thermal dose maps are shown in Fig. 12. Contrast-enhanced-images were obtained in each canine following completion of treatment for visualization of non-perfused volume (Fig. 12g). Real-time assessment of thermal dose provided ablation volume estimates during treatment are displayed in Fig. 12e and Fig. 12f. In all specimens, regions of thermocoagulation were detected and noted to be within the prostate capsule, with no thermal damage to the peri-prostatic tissues (Table 1).

In all canines erectile responses were evaluated with a cavernous nerve stimulator in average 5 days (range 0 to 15 days) post-treatment and showed tumescence responses≥2 on an ordinal scale ranging from +2 to +4 after a stimulation with a maximum current of 14 mA (Table 1). These results indicated intact cavernous nerve functionality.

Additionally, ablated volumes defined by cumulative thermal dose and volumes identified on post-procedural contrast-enhanced MRI demonstrated excellent correlation on visual analysis. All of the ablation zones received a consensus score of 3 (excellent) for the location and size of the correlation between the histologic ablation zone and MRI based ablation zone during the review of the lesions by a genitourinary pathologist and radiologist (Table 1). During the prostatectomy and histologic examination, no damage was noted in the bladder and rectum.

Discussion

Image guided focal therapy for Pca represents an evolving paradigm shift that may achieve reliable oncologic efficacy with minimal morbidity. Emerging novel focal or regional ablative therapies include laser ablation, cryotherapy, electroporation and HIFU [4]. The use of ablative hyperthermia for treatment of Pca may be efficacious[4], and many trials have demonstrated the value of HIFU in cancer control[6, 12, 24, 25].

Ultrasound Therapy

Trans-urethral ultrasound therapy has considerable potential predicted by prior successes employing trans-rectal HIFU as focal treatment[4, 6, 12]. While it is estimated that up to 80% of Pca is multifocal in nature, it is believed that not all lesions are equivalent in terms of their propensity to grow and metastasize. Although controversial, the existence of a dominant index lesion responsible for cancer progression and metastasis has been proposed by many experts[26]. Given recent controversies concerning potential overtreatment of clinically insignificant disease, targeted treatment of an index lesion may be a viable and practical solution[4, 26]. In this case, focal and/or regional treatment may be effective as a cancer control modality.

Limitations of trans-rectal ultrasound (TRUS) imaging and TRUS biopsy have been well documented [27]. Multi-parametric MRI has been shown to be superior to that of TRUS biopsy in the detection of Pca [28]. Furthermore, some studies have demonstrated cancer detection specificity and sensitivity as high as 0.94 and 0.84 for T_2-weighted MRI alone, significantly improving when multiple parameters are combined [29]. Coupling multi-parametric MRI with a trans-urethral ultrasound therapy device may allow for accurate diagnosis, targeting, and treatment of cancer foci [13].

Our results in a canine model suggest that MR-guided trans-urethral ultrasound therapy is a safe and feasible technique, allowing for spatially accurate and precise ablation of prostate tissue without damaging the neurovascular bundle and the surrounding organs. The nerves around the prostate responsible for erection remained functionally and anatomically intact following HIFU treatment. Using real-time multi-planar and multi-slice temperature monitoring with automated temperature feedback

control, it is possible to reach ablative temperatures in targeted regions, while avoiding excess temperature elevation in critical anatomical areas. In this study, target locations were located in the central zone, transition zone, and peripheral zone, demonstrating adequate sonication depth in treatment of all lesions in the prostate. It is critical to achieve effective, targeted treatment of peripheral Pca lesions while avoiding extra-prostatic thermal damage, given that the majority of Pca lesions reside in the peripheral zone and the proximity of these tumors to the neurovascular bundles. Maintaining the integrity of vulnerable regional anatomy while achieving oncologic efficacy will be one of the main objectives when translating trans-urethral MR-guided ultrasound therapy to clinical care.

Although these results are encouraging, further experiments are needed to optimize trans-urethral MR-guided ultrasound therapy for use in humans. In these initial experiments, the transducer was rigid and remained stationary during sonications. However, since the applicator can be rotated and the transducer elements can be individually activated and power modulated, the system does have the flexibility to perform either regional or whole gland ablations, allowing precise control of ablation[30, 31]. Future experiments can take advantage of particularly the rotational control: rotating the transducer while sonicating may allow for larger ablation volumes in a shorter time period, as validated by other groups[30, 32]. Moreover, a flexible ultrasound applicator could facilitate urethral placement similarly to a Foley urethral catheter. We recommend post-pubertal canines for future pre-clinical ultrasound therapy studies of the prostate to assure large enough prostate sizes for treatment of multiple locations. This thermoablative therapy could potentially be applied to the treatment of benign prostatic hypertrophy. The potential and flexibility of this trans-urethral device to rapidly provide focal, regional, or whole-gland therapy is attractive in comparison to other Pca therapy devices.

Limitations in this study include performing only one ablation in each target region, which fails to fully simulate a clinical procedure, in which multiple ablations (or a

continuous ablation utilizing rotational control) are targeted upon a single cancerous region creating a tumor-free treatment margin. Moreover, the short-term or long-term outcomes of trans-urethral ultrasound ablations were not assessed in this study.

In summary, coupling MRI with a trans-urethral ultrasound therapy device enabled multi-planar temperature monitoring at the target region as well as in surrounding tissues, allowing for safe, targeted, and controlled ablations of prescribed prostatic lesions in a canine model. There was no impact of ablation on the function of the neurovascular bundle and surrounding organs such as rectum and bladder. Functionality of the cavernosal nerves after trans-urethral ultrasound therapy was confirmed with a nerve stimulator measuring the tumescence response. These preliminary data underscore the value of future clinical studies to confirm the feasibility, safety, oncologic control, and functional outcomes of this treatment for Pca.

Acknowledgements

We would like to thank our MRI technologists S. Peters and E. Jamison as well as the veterinarian technicians J. Vosicky, M. Brunner, K. Peterson, J. McGrath, and M. Zamora for their outstanding support of this study and Dr. D. Mustafi for providing degassed water.

Comments

(1) Background

Prostate cancer is the second most common cancer and among the leading causes of cancer deaths in men in the US. There is a growing interest in targeted treatment strategies for prostate cancer that could achieve comparable effects to standard surgical treatments with minimal adverse effects on sexual and urinary function. Therapeutic ultrasound therapy is an emerging, minimally invasive treatment option where an ultrasound probe emits a focused high intensity beam that can be used to destroy or "ablate" cancerous tissue. This study evaluated the feasibility of using a novel ultrasound therapy device combined with real-time magnetic resonance imaging (MRI) guidance to ablate prostate tissue in vivo.

(2) Research frontiers

In our study, a transurethral ultrasound therapy device combined with real-time MRI based temperature monitoring was tested in a preclinical canine model. We evaluated the feasibility and safety of MRI-guided trans-urethral ultrasound to effectively and accurately ablate prostate tissue while minimizing the damage to surrounding tissues in canine prostate. In addition to assessing rectal and bladder damage, we specifically assessed the post-treatment functionality of the nerves by analyzing their response qualitatively and quantitatively with a nerve stimulator.

(3) Innovations and breakthroughs

In this study, MRI images enabled identification of the prostate and planning of the ultrasound therapy locations in all canines. Prostate tissue was successfully ablated with the MRI-guided ultrasound therapy unit and regions of tissue destruction were found to be within the prostate capsule, with no thermal damage to the tissues surrounding the prostate. In all canines erectile responses were evaluated with a nerve stimulator post-treatment and indicated intact nerve functionality. No damage was

noted in the bladder and rectum.

(4) Applications

Image guided focal therapy for prostate cancer represents an evolving paradigm shift that may be able to treat prostate cancer with fewer side effects than standard treatments. Our results in a canine model suggest that MRI-guided trans-urethral focal ultrasound therapy is a safe and feasible technique, allowing for spatially accurate and precise ablation of prostate tissue without damaging the neurovascular bundle and the surrounding organs.

(5) Terminology

Thermo-ablation: Absorption of (ultrasound) energy that creates an increase in temperature and destroys tissue when the temperature exceeds ≥56°C within the focal area.

Thermocoagulation: The use of heat to bring about localized destruction and congealing of tissue.

Transurethral: A medical procedure performed via the urethra.

Neurovascular bundle: The nerves, arteries, veins and lymphatics that travel together in the body, specifically in this article, around the prostate.

Cavernous Nerve: The nerves that facilitate penile erection

(6) Peer review

References

1 ACS. American Cancer Society. Cancer Facts & Figures 2014. *American Cancer Society* 2014

2 Klotz L. Prostate cancer overdiagnosis and overtreatment. *Current opinion in endocrinology, diabetes, and obesity* 2013; **20**(3): 204-209 [PMID: 23609043 DOI: 10.1097/MED.0b013e328360332a]

3 Hoang AN, Volkin D, Yerram NK, Vourganti S, Nix J, Linehan WM, Wood B, Pinto PA. Image guidance in the focal treatment of prostate cancer. *Current opinion in urology* 2012; **22**(4): 328-335 [PMID: 22647649 DOI: 10.1097/MOU.0b013e32835482cc]

4 Lindner U, Trachtenberg J, Lawrentschuk N. Focal therapy in prostate cancer: modalities, findings and future considerations. *Nature reviews Urology* 2010; **7**(10): 562-571 [PMID: 20842187 DOI: 10.1038/nrurol.2010.142]

5 Hildebrandt B, Wust P, Ahlers O, Dieing A, Sreenivasa G, Kerner T, Felix R, Riess H. The cellular and molecular basis of hyperthermia. *Critical reviews in oncology/hematology* 2002; **43**(1): 33-56 [PMID: 12098606]

6 Ahmed HU, Freeman A, Kirkham A, Sahu M, Scott R, Allen C, Van der Meulen J, Emberton M. Focal therapy for localized prostate cancer: a phase I/II trial. *The Journal of urology* 2011; **185**(4): 1246-1254 [PMID: 21334018 DOI: 10.1016/j.juro.2010.11.079]

7 Lindner U, Lawrentschuk N, Weersink RA, Davidson SR, Raz O, Hlasny E, Langer DL, Gertner MR, Van der Kwast T, Haider MA, Trachtenberg J. Focal laser ablation for prostate cancer followed by radical prostatectomy: validation of focal therapy and imaging accuracy. *Eur Urol* 2010; **57**(6): 1111-1114 [PMID: 20346578 DOI: S0302-2838(10)00226-5 [pii]

10.1016/j.eururo.2010.03.008]

8 Lukka H, Waldron T, Chin J, Mayhew L, Warde P, Winquist E, Rodrigues G, Shayegan B, Genitourinary Cancer Disease Site Group of Cancer Care Ontario's Program in Evidence-Based C. High-intensity focused ultrasound for prostate cancer: a systematic review. *Clinical oncology* 2011; **23**(2): 117-127 [PMID: 20932728 DOI: 10.1016/j.clon.2010.09.002]

9 Soylu FN, Eggener S, Oto A. Local staging of prostate cancer with MRI. *Diagnostic and interventional radiology* 2012; **18**(4): 365-373 [PMID: 22399364 DOI: 10.4261/1305-3825.DIR.4970-11.2]

10 Jia G, Abaza R, Williams JD, Zynger DL, Zhou J, Shah ZK, Patel M, Sammet S, Wei L, Bahnson RR, Knopp MV. Amide proton transfer MR imaging of prostate cancer: a preliminary study. *Journal of magnetic resonance imaging : JMRI* 2011; **33**(3): 647-654 [PMID: 21563248 PMCID: 4287206 DOI: 10.1002/jmri.22480]

11 Wang S, Peng Y, Medved M, Yousuf AN, Ivancevic MK, Karademir I, Jiang Y, Antic T, Sammet S, Oto A, Karczmar GS. Hybrid multidimensional T(2) and diffusion-weighted MRI for prostate cancer detection. *Journal of magnetic resonance imaging : JMRI* 2014; **39**(4): 781-788 [PMID: 23908146 PMCID: 4251798 DOI: 10.1002/jmri.24212]

12 Ahmed HU, Hindley RG, Dickinson L, Freeman A, Kirkham AP, Sahu M, Scott R, Allen C, Van der Meulen J, Emberton M. Focal therapy for localised unifocal and multifocal prostate cancer: a prospective development study. *Lancet Oncol* 2012 [PMID: 22512844 DOI: S1470-2045(12)70121-3 [pii]

10.1016/S1470-2045(12)70121-3]

13 Partanen A, Yerram NK, Trivedi H, Dreher MR, Oila J, Hoang AN, Volkin D, Nix J, Turkbey B, Bernardo M, Haines DC, Benjamin CJ, Linehan WM, Choyke P, Wood BJ, Ehnholm GJ, Venkatesan AM, Pinto PA. Magnetic resonance imaging (MRI)-guided transurethral ultrasound therapy of the prostate: a preclinical study with radiological and pathological correlation using customised MRI-based moulds. *BJU international* 2013; **112**(4): 508-516 [PMID: 23746198 PMCID: 3816743 DOI: 10.1111/bju.12126]

14 Meshorer A, Prionas SD, Fajardo LF, Meyer JL, Hahn GM, Martinez AA. The effects of hyperthermia on normal mesenchymal tissues. Application of a histologic grading system. *Archives of pathology & laboratory medicine* 1983; **107**(6): 328-334 [PMID: 6687797]

15 Ishihara Y, Calderon A, Watanabe H, Okamoto K, Suzuki Y, Kuroda K, Suzuki Y. A precise and fast temperature mapping using water proton chemical shift. *Magnetic resonance in medicine : official journal of the Society of Magnetic Resonance in Medicine / Society of Magnetic Resonance in Medicine* 1995; **34**(6): 814-823 [PMID: 8598808]

16 Chen J, Daniel BL, Diederich CJ, Bouley DM, van den Bosch MA, Kinsey AM, Sommer G, Pauly KB. Monitoring prostate thermal therapy with diffusion-weighted MRI. *Magnetic resonance in medicine : official journal of the Society of Magnetic Resonance in Medicine / Society of Magnetic Resonance in Medicine* 2008; **59**(6): 1365-1372 [PMID: 18506801 DOI: 10.1002/mrm.21589]

17 Jacobs MA, Herskovits EH, Kim HS. Uterine fibroids: diffusion-weighted MR imaging for monitoring therapy with focused ultrasound surgery--preliminary study. *Radiology* 2005; **236**(1): 196-203 [PMID: 15987974 DOI: 10.1148/radiol.2361040312]

18 Chopra R, Tang K, Burtnyk M, Boyes A, Sugar L, Appu S, Klotz L, Bronskill M. Analysis of the spatial and temporal accuracy of heating in the prostate gland using transurethral ultrasound therapy and active MR temperature feedback. *Physics in medicine and biology* 2009; **54**(9): 2615-2633 [PMID: 19351975 DOI: 10.1088/0031-9155/54/9/002]

19 Kim HL, Mhoon DA, Brendler CB. Does the CaverMap device help preserve potency? *Current urology reports* 2001; **2**(3): 214-217 [PMID: 12084267]

20 Walsh PC, Marschke P, Catalona WJ, Lepor H, Martin S, Myers RP, Steiner MS. Efficacy of first-generation Cavermap to verify location and function of cavernous nerves during radical prostatectomy: a multi-institutional evaluation by experienced surgeons. *Urology* 2001; **57**(3): 491-494 [PMID: 11248626]

21 Makin CA, Bobrow LG, Bodmer WF. Monoclonal antibody to cytokeratin for use in routine histopathology. *J Clin Pathol* 1984; **37**(9): 975-983 [PMID: 6206100 PMCID: 498911]

22 Van Leenders GJ, Beerlage HP, Ruijter ET, de la Rosette JJ, van de Kaa CA. Histopathological changes associated with high intensity focused ultrasound (HIFU) treatment for localised adenocarcinoma of the prostate. *J Clin Pathol* 2000; **53**(5): 391-394 [PMID: 10889823 PMCID: 1731195]

23 Sapareto SA, Dewey WC. Thermal dose determination in cancer therapy. *International journal of radiation oncology, biology, physics* 1984; **10**(6): 787-800 [PMID: 6547421]

24 Foster RS, Bihrle R, Sanghvi N, Fry F, Kopecky K, Regan J, Eble J, Hennige C, Hennige LV, Donohue JP. Production of prostatic lesions in canines using transrectally administered high-intensity focused ultrasound. *European urology* 1993; **23**(2): 330-336 [PMID: 7683997]

25 Gelet A, Chapelon JY, Margonari J, Theillere Y, Gorry F, Cathignol D, Blanc E. Prostatic tissue destruction by high-intensity focused ultrasound: experimentation on canine prostate. *Journal of endourology / Endourological Society* 1993; **7**(3): 249-253 [PMID: 8358423]

26 Ahmed HU. The index lesion and the origin of prostate cancer. *The New England journal of medicine* 2009; **361**(17): 1704-1706 [PMID: 19846858 DOI: 10.1056/NEJMcibr0905562]

27 Hwang SI, Lee HJ. The future perspectives in transrectal prostate ultrasound guided biopsy. *Prostate international* 2014; **2**(4): 153-160 [PMID: 25599070 PMCID: 4286726 DOI: 10.12954/PI.14062]

28 Sciarra A, Barentsz J, Bjartell A, Eastham J, Hricak H, Panebianco V, Witjes JA. Advances in magnetic resonance imaging: how they are changing the management of prostate cancer. *European urology* 2011; **59**(6): 962-977 [PMID: 21367519 DOI: 10.1016/j.eururo.2011.02.034]

29 Turkbey B, Pinto PA, Mani H, Bernardo M, Pang Y, McKinney YL, Khurana K, Ravizzini GC, Albert PS, Merino MJ, Choyke PL. Prostate cancer: value of multiparametric MR imaging at 3 T for detection--histopathologic correlation. *Radiology* 2010; **255**(1): 89-99 [PMID: 20308447 PMCID: 2843833 DOI: 10.1148/radiol.09090475]

30 Chopra R, Colquhoun A, Burtnyk M, N'Djin W A, Kobelevskiy I, Boyes A, Siddiqui K, Foster H, Sugar L, Haider MA, Bronskill M, Klotz L. MR imaging-controlled transurethral ultrasound therapy for conformal treatment of prostate tissue: initial feasibility in humans. *Radiology* 2012; **265**(1): 303-313 [PMID: 22929332 DOI: 10.1148/radiol.12112263]

31 Diederich CJ, Stafford RJ, Nau WH, Burdette EC, Price RE, Hazle JD. Transurethral ultrasound applicators with directional heating patterns for prostate thermal therapy: in vivo evaluation using magnetic resonance thermometry. *Medical physics* 2004; **31**(2): 405-413 [PMID: 15000627]

32 Siddiqui K, Chopra R, Vedula S, Sugar L, Haider M, Boyes A, Musquera M, Bronskill M, Klotz L. MRI-guided transurethral ultrasound therapy of the prostate gland using real-time thermal mapping: initial studies. *Urology* 2010; **76**(6): 1506-1511 [PMID: 20709381 DOI: 10.1016/j.urology.2010.04.046]

Tables

Table 1: Intra- and post-surgical evaluations after the treatment of eight canines prostates in-vivo with MRI guided ultrasound therapy: tumescence response on an ordinal scale, assessment of thermal damage to peri-prostatic tissues, and correlation between MRI and pathology for location and size of the ablation zone.

Canine #	Tumescence response	Inspection of peri-prostatic tissues	Correlation between MRI and pathology for location and size of the ablation zone (no correlation: 1; modest correlation: 2; and excellent correlation: 3)
1	3	no damage	3
2	4	no damage	3
3	3	no damage	3
4	2	no damage	3
5	4	no damage	3
6	2	no damage	3
7	3	no damage	3
8	3	no damage	3

Figure Legends

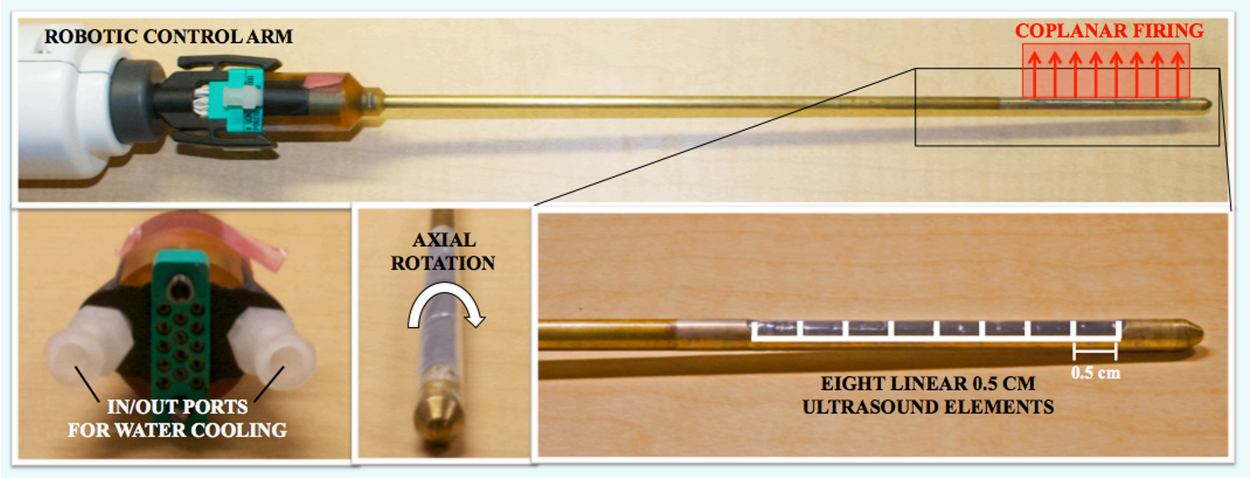

Figure 1 Trans-urethral ultrasound therapy probe. Rigid, water-cooled trans-urethral ultrasound applicator (5 mm [15 French] diameter) with eight transducer elements (4mm × 5 mm/element). A motor unit with a robotic control arm allows rotation of the water-cooled applicator around the long axis.

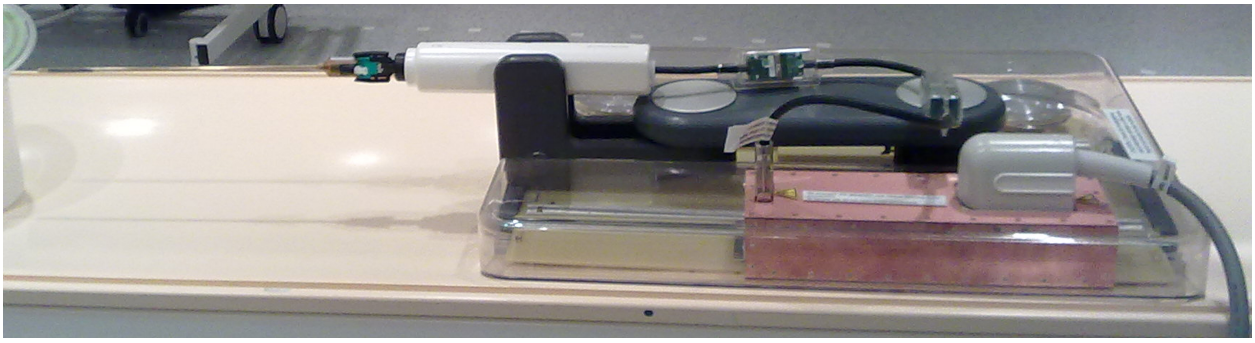

Figure 2 MRI-compatible ultrasound therapy device. Set-up of the trans-urethral ultrasound applicator (left) on the MRI patient table with control cables, control box and motor unit to control the rotation of the ultrasound transducer (right).

Figure 3 Equipment integration for MRI-guided ultrasound therapy. Frontal oblique view of the 3T Philips MRI scanner with an 8-channel cardiac MR coil on the anterior part of the scanner table and ultrasound transducer on the posterior part of scanner table.

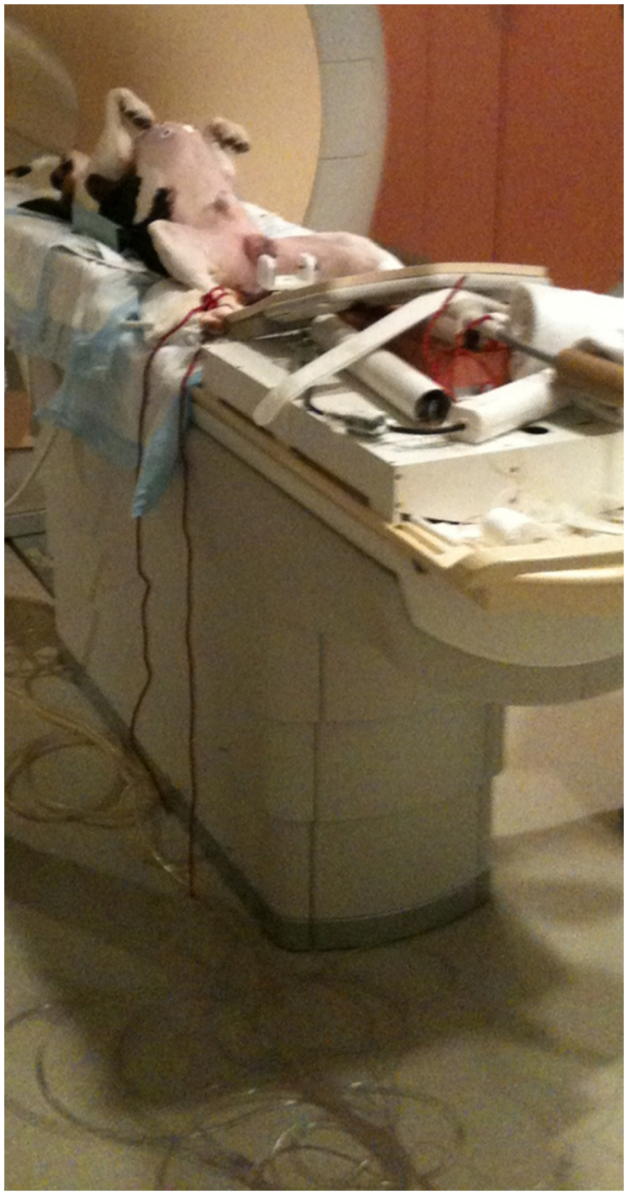

Figure 4 Canine positioning for MRI-guided ultrasound treatment. Positioning of a canine in supine orientation on the patient table and placement of the transurethral ultrasound transducer in the canine prostate.

Figure 5 The CaverMap Surgical Aid nerve stimulator control unit. Device control unit with connectors for the stimulation needle, display of the applied current in mA, and LED display (blue and red) to visualize tumescence response on an ordinal scale.

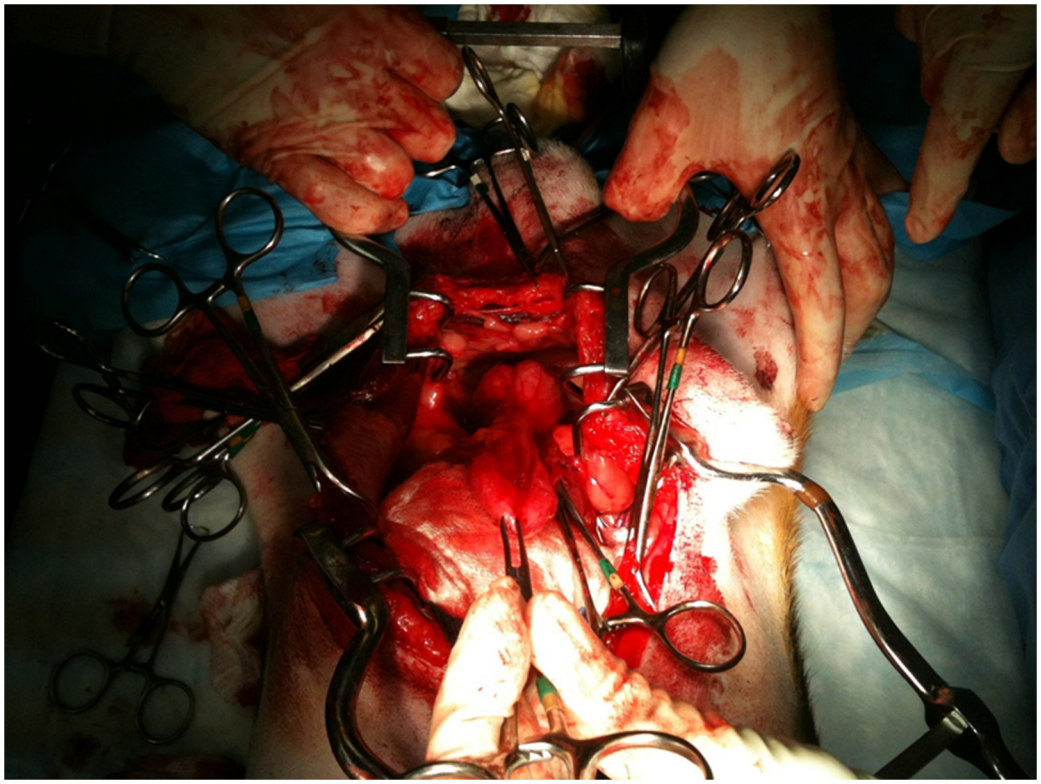

Figure 6 Surgical preparation of the canine prostate for nerve stimulation of the cavernosal nerves.

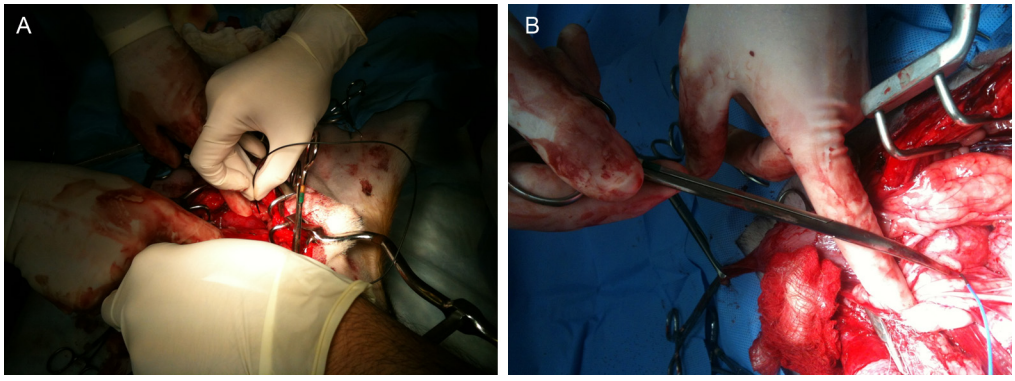

Figure 7A and B Placement of the CaverMap Surgical Aid nerve stimulator. Intrasurgical placement of the stimulation needle of the CaverMap Surgical Aid nerve stimulator close to the cavernosal nerves of the canine prostate.

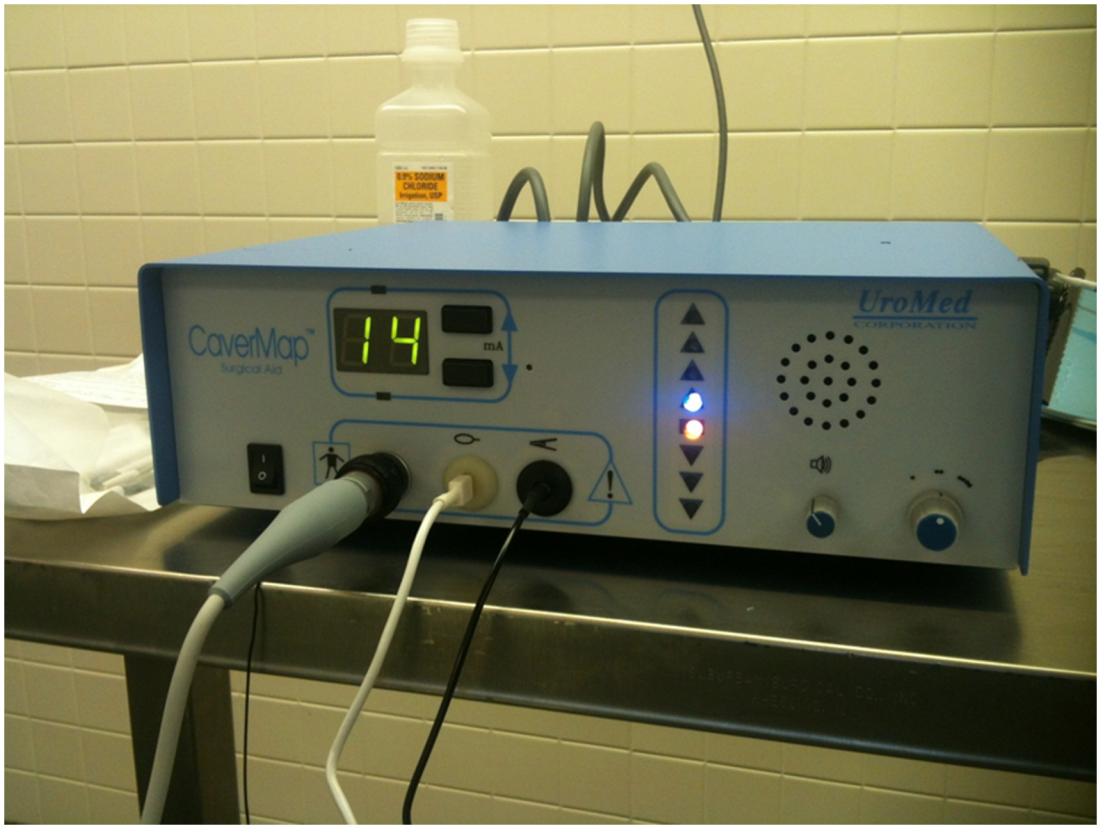

Figure 8 The CaverMap Surgical Aid nerve stimulator display. Control unit and display of the CaverMap Surgical Aid nerve stimulator to measure tumescence response on an ordinal scale intraoperatively. Below the digital display are the connectors for the probe handle, the tumescence sensor, and the lead that connects the sensor to the control unit. The electrode containing probe tip emits the electrical current.

Figure 9 Explanted canine prostate and bladder after prostatectomy.

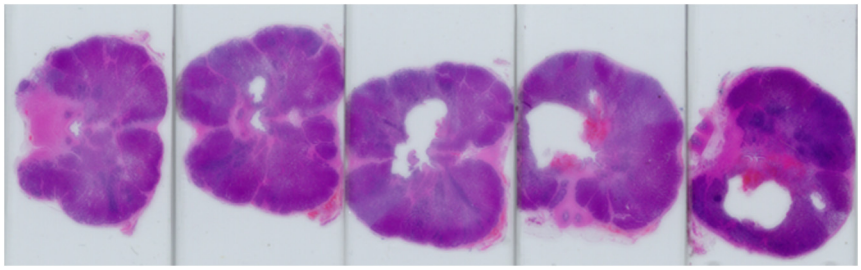

Figure 10 Histology of treated canine prostate. Series of histological slides of a canine prostate after H&E staining show grossly visible lesions.

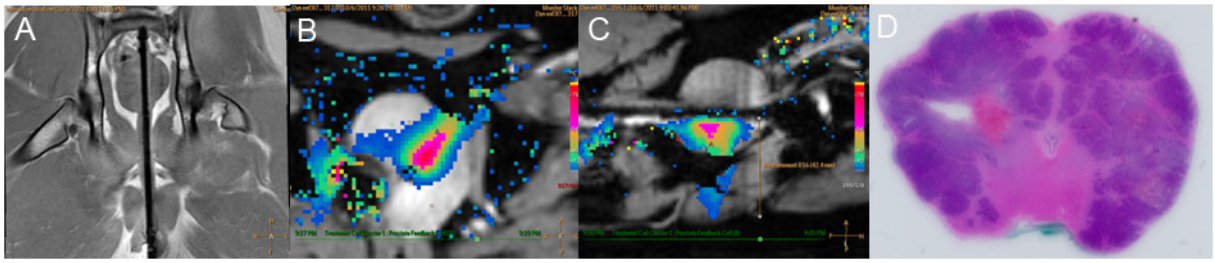

Figure 11 Example images of planning, treatment, and histological outcome. A: Coronal MR image of the intra-urethral catheter placement in the canine prostate for treatment planning with the canine in supine position: The ultrasound applicator is advanced along the urethra to the level of the prostate, **B:** Color-coded axial temperature map overlaid on dynamic magnitude images during a sonication showing typical temperature distribution at the end of a sonication. Temperature monitoring and control was achieved in the target location with an FFE-EPI imaging sequence, utilizing the PRFS- method for temperature mapping, and by using a binary temperature feedback algorithm, **C:** saggital temperature map during HIFU treatment, **D:** histological slide of the canine prostate in haematoxylin and eosin staining to evaluate HIFU treatment effects.

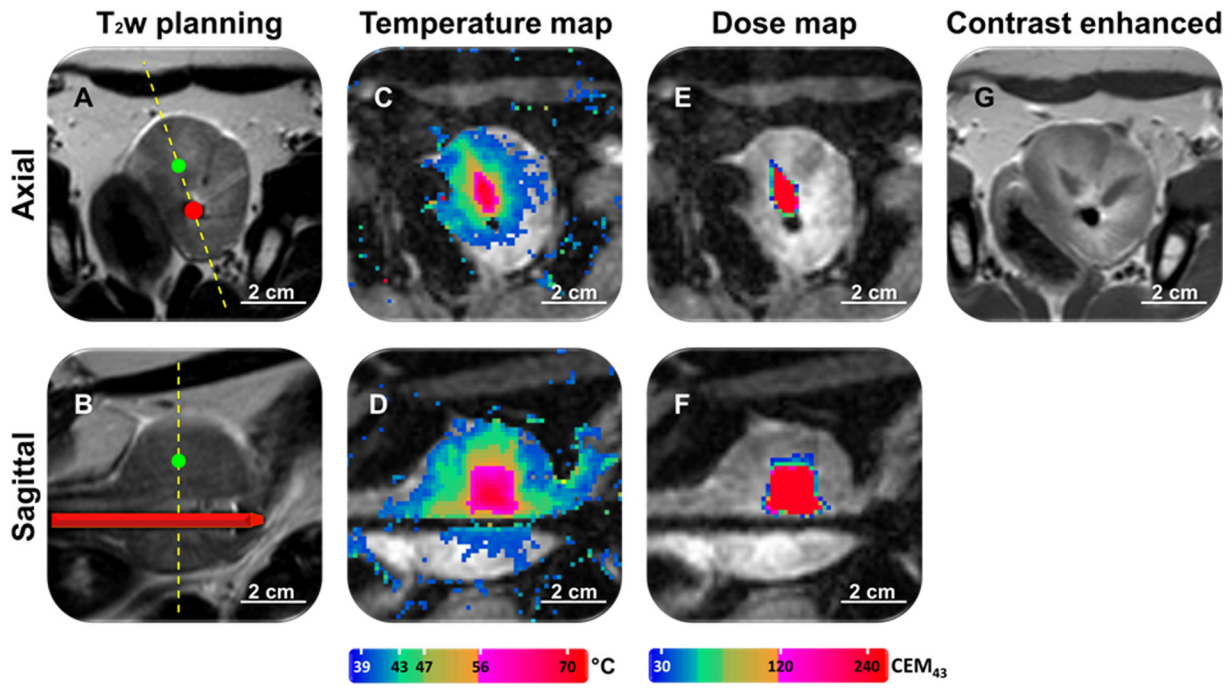

Figure 12 Representative images of MRI-Guidance. A: T_2-weighted image for positioning and treatment planning in axial and **B:** saggital orientation, **C:** MR temperature map during ultrasound treatment in axial and **D:** saggital orientation. **E:** MR dose map during ultrasound treatment in axial and **F:** saggital orientation. **G:** Contrast enhanced T_1-weighted image after ultrasound treatment.